ORIGINAL CONTRIBUTION

Compression behaviors of magnetorheological fluids under nonuniform magnetic field

Chaoyang Guo · Xinglong Gong · Shouhu Xuan · Lijun Qin · Qifan Yan

Abstract This work is concerned with an experimental and theoretical study on compression properties of magnetorheological fluids under the nonuniform field. Experimental tests of unidirectional monotonic compression were firstly carried out under constant area operation using a commercial plate–plate magneto-rheometer where the magnetic field radial distribution was nonuniform. Normal forces increased with decreasing of the gap distance, and two regions were found through the normal force versus gap distance curves: elastic deformation and plastic flow. High normal forces could be obtained in the case of high magnetic field, high compression velocity, low initial gap distance, high volume fraction, and high medium viscosity. In the plastic flow region, the normal force with the gap distance could be fitted with a power law relation $F_N \propto h^n$, and the index n was around well in the range $(-3, -2)$. Taking nonuniform magnetic field into account, the theoretical modeling in the plastic flow was then developed to calculate the normal force under compression based on the continuum media theory. Compared to the uniform field, there existed a magnetic field gradient-induced normal force under nonuniform field. Considering the sealing and squeeze strengthening effect, the gap distance-dependent shear yield stress was proposed, and a good correspondence between the theoretical and experimental results was obtained.

Introduction

Magnetorheological (MR) fluids are suspensions of magnetic microparticles in a carrier fluid, which present dramatic changes in the rheological properties under magnetic field. Because of their fast and reversible response, high changeable shear yield stress, MR fluids have attracted many attentions in many fields of science and engineering (Ashour et al. 1996; Carlson and Jolly 2000; Bossis et al. 2002; Park et al. 2010; de Vicente et al. 2011a). As the important parameter of MR fluid, high shear yield stress of MR fluids is expected, since it means a smaller MR device in the same output force. Therefore, compression or squeeze mode of MR fluids has been considered recently, as it has been proved that the compression mode of MR fluids can provide higher yield stress than the direct-shear and pressure-driven mode, which is similar to the reported studies using electrorheological (ER) fluids, an analogue of MR fluid (Havelka and Pialet 1996; Chu et al. 2000; Tian et al. 2002a, b, 2003).

The first report on compression behaviors of MR fluids is the squeeze strengthening effect (Tang et al. 2000; Zhang et al. 2004). A higher yield stress could be obtained under compression for the MR fluids, which was relative to the formation of thick strong columns under compression and friction effect between the particles. Similar to the ER fluids, the investigation of the compression behaviors for the MR fluids could be also divided into two categories. The first one was the oscillatory compression mode, in which the gap distance between the plates changed in sinusoidal mode,

C. Guo · X. Gong (✉) · S. Xuan (✉) · L. Qin · Q. Yan
Department of Modern Mechanics, CAS Key Laboratory of Mechanical Behavior and Design of Materials, University of Science and Technology of China, Hefei, 230027, China
e-mail: gongxl@ustc.edu.cn; xuansh@ustc.edu.cn

and the oscillatory amplitude was only a few percentage of the initial gap distance. Kulkarni et al. (2003) studied the hysteretic loops of the MR fluids under oscillatory squeeze mode. The results indicated that the damping force and the area of the hysteretic loop of MR fluids increased with the current and strain amplitude. However, the introduction of a squeeze component in shearing flows did not always increase the strength of the MR fluid. Furthermore, Vieira et al. (2003) found that the peak compressive force increased with increasing of the cycle numbers. Well-pronounced hysteresis loops were observed by Gstöttenbauer et al. (2008), and they exhibited characteristic kinks, which could not be understood within the frame of elementary constitutive laws. Finite element simulations were utilized to describe the squeeze mode behavior. Farjoud et al. (2011, 2012) and Zhang et al. (2011) did a great job to develop the practical MR squeeze mount. Besides, a clumping behavior was observed during the oscillatory testing and a novel mathematical solution for low shear rate squeezing flow of MR fluids was made using perturbation techniques.

The other investigation method for the compression mode was the unidirectional monotonous compression. The reduction in the plate could be achieved to a large extent, but the squeezing velocity was often limited to a small constant value. By comparing the steady shear flow and constant velocity squeezing flow behaviors of the MR fluid, See (2003a) found that the mechanical response under squeezing flow scaled as $B^{0.91}$, whereas the response under shearing scaled as $B^{1.4}$. Mazlan et al. (2007, 2008) designed a test rig to perform the constant velocity and area compression operation of MR fluids, and three regions were found through the stress–strain curves, which was relative to the relative movement between the particles and the carrier liquid in the MR fluid. Similar tests were also conducted by Wang et al. (2011), and the results showed that the MR fluid was quite stiff at small compressive strains lower than 0.13. The compressive stress and the compressive modulus increased quickly when the compressive strain was higher than 0.2. To avoid the sealing effect under constant area squeeze, de Vicente et al. (2011b), Ruiz-López et al. (2012) investigated the unidirectional monotonic compression tests of MR fluids under constant volume operation. They proposed a unified description for the MR fluids in terms of a continuous media theory for plastic materials. This allowed them to collapse compression curves obtained for a wide range of magnetic field strengths, medium viscosity, and particle concentration. In addition, particle-level dynamic simulations were made to capture the microstructure revolution of MR fluid under compression.

Different from the electric field, the magnetic field distribution with the radial direction produced by the coil is hard to keep uniform. For all the reported self-assembled device (Kulkarni et al. 2003; Vieira et al. 2003; Mazlan et al. 2007;

2008; Wang et al. 2011) and commercial setup (Laeuger et al. 2005; Laun et al. 2008a; López-López et al. 2010; Andablo-Reyes et al. 2011; Jonkkari et al. 2012), the radial magnetic fields were not uniform, and the magnetic field gradient always existed under a given current. The nonuniform field would change the properties of field-responsive materials greatly; López-López et al. (2010) found that the lack of homogeneity of the applied field could cause the appearance of normal forces in MR fluids, and Andablo-Reyes et al. (2011) discovered that the nonuniform field could affect the lubrication behaviors of magnetic fluids. Therefore, the compression properties of MR fluids are inevitably affected by this nonuniform field. However, compression behaviors of MR fluids under nonuniform field have been not studied.

In this work, the compression properties of MR fluids under nonuniform magnetic field were investigated by using a commercial plate–plate rheometer. The influence factors including magnetic field, compression velocity, initial gap distance, volume concentration of iron particle, and the viscosity of carrier fluid were systematically investigated in the compression mode. Considering the nonuniform magnetic field, the theoretical model was carried out based on a continuum media theory to calculate the normal force, and the comparison between the nonuniform and uniform fields was made. Besides, the gap distance-dependent yield stress was utilized, and they showed good agreements with the experimental results.

Experimental

MR fluids used in this study were prepared by mixing carbonyl iron particles in silicone oil. The carbonyl iron particles were purchased from BASF (model CN) whose average particle size was about 6 μm. Silicone oil (H201) was purchased from Sinopharm Chemical Reagent Co., Ltd. Stearic acid (2 wt %) was added to improve sedimentary stability. Various samples with different iron particle volume fractions (5–25 %) and viscosity of carrier fluid (10, 100, and 500 cSt) were prepared. The samples were vigorously shaken to ensure the required homogeneity before measurements.

The commercial plate–plate magneto-rheometer (Physica MCR 301; Anton Paar, Austria) was used to test the compression behaviors of MR fluids. The magnetic field was applied normally to the sample plate via the magnetorheological unit (Physica MRD 180). The normal force was measured with a sensor built into air bearing, and it could be recorded from −50 to 50 N with an accuracy of 0.03 N. The rheometer axis stiffness was very large (2 N/μm), and the distortion of the force sensor under the pressures was neglected. The inertia of the plate tool
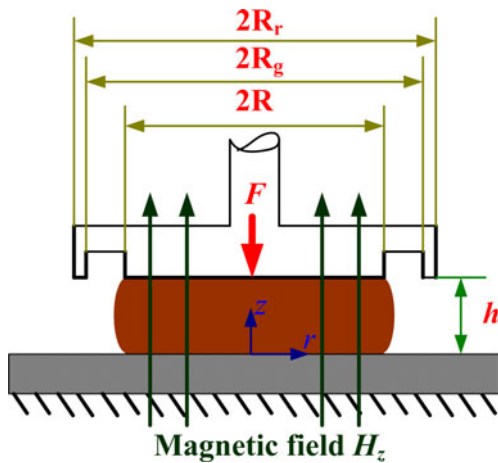
Fig. 1 Schematic diagram of the constant area compression experiment

was also ignored. The plates were assumed to be perfectly parallel, even though a small misalignment existed (Andablo-Reyes et al. 2011; Gong et al. 2012), as it was so small compared to the gap distance.

The schematic diagram of the compression test is shown in Fig. 1. During compressing, the lower plate is stationary, while the upper plate moves close to it with a constant velocity, and MR fluids are pushed out. It should be noted that the upper plate is not an ideal cylindrical plate, and there is an additional guard ring. To keep a constant area, the extrusive MR fluids cannot touch the guard ring. In the initial state, the MR fluid is fully filled between the middle surface of the upper and lower plates. The radius and height of the sample is R (10 mm) and h_0. When the MR fluid just can touch the guard ring, the radius and height of the sample is R_g (13 mm) and h_1. During compressing, the volume of sample keeps constant, that is $\pi R^2 h_0 = \pi R_g^2 h_1$ (supposing the sample is the cylinder). We define the compression strain as the ratio of the moving distance of the upper plate to the initial distance between the plates as follows: $\varepsilon_c = (h_0 - h(t))/h_0$, where $h(t)$ is the transient height during compressing. Therefore, a maximum compression strain cannot exceed the value of 0.408.

The distribution of the magnetic field in the measuring gap for each given electric current is not uniform, and a nonnegligible gradient along the radial coordinate exists. Figure 2 represents the magnetic field distribution in the testing gap as a function of radial distance without sample. The middle magnetic field is smaller than that in the neighborhood as a central hole exists to pass through the rheometer shaft. The field distribution for the different sample is a little different, but the field gradient always exists. Obviously, the magnetic field will be changed as the gap distance decreases. This small change for magnetic field has been ignored, and the magnetic field distribution is thought

as a constant value during compressing. During the testing process, the radial field gradient exists, and the mentioned magnetic flux density in this paper refers to the maximum plateau value corresponding to radial magnetic flux density profiles.

Compression measurements were carried out as follows: (1) samples were placed between the parallel plates with a syringe, and different initial gap distances demanded different volume samples. (2) The external magnetic field was suddenly applied for 60 s, while the sample kept stationary which was long enough to allow the aggregates to form. (3) The compression test was started at a constant approaching speed in the presence of the nonuniform magnetic field. All the tests were repeated for three times to guarantee the validity of the results (every testing result almost overlapped in one line, and the relative error was less than 1 %), and the testing temperature was set at 25 °C.

Results

The general feature of normal force tested under the nonuniform magnetic field

Firstly, the compression tests were carried out without applying magnetic field, which indicated that all the normal force was less than 0.1 N; thus, it was discarded for brevity. Then, experimental tests were conducted under constant current to test the magnetic-dependent normal force. Here, it should be noted that all the tests were under the nonuniform field with the steady field distribution. Figure 3 shows a typical behavior of a normal force of MR fluid under compression with the gap distance and strain. Though the MR fluid is not subject to any deformation after applying a magnetic field, the positive normal force generates (3.38 N) and pushes the plates apart, which is marked by the red star in Fig. 3. The static normal force has been
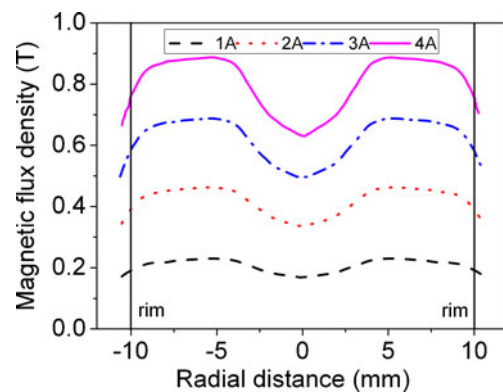
Fig. 2 The magnetic field distribution in the testing gap as a function of radial distance

studied by many researchers (See and Tanner 2003b; Laun et al. 2008b; López-López et al. 2010; Gong et al. 2012), and it originates from the squeezing of magnetized spheres into existing chains. The static normal force F_{NS} is mainly dependent on the magnetic field B by the power law relation $F_{NS} \propto B^k$, where k is about 2. In modeling the normal force under compression, this static field should be included. It should be also noted that the initial gap becomes a little larger (it increases from 0.625 to 0.627 mm) as this static normal force causes the rheometer axis distortion.
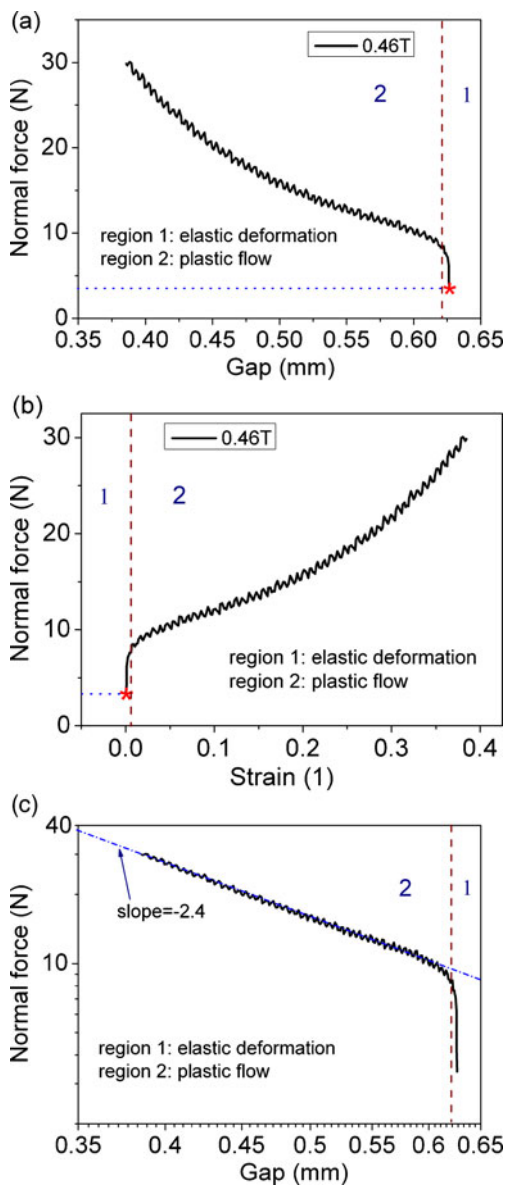
Fig. 3 Normal force of MR fluid versus **a** gap distance in lin–lin plot, **b** strain in lin–lin plot, and **c** gap distance in log–log plot under compression. The particle volume fraction of MR fluid is 10 %, the viscosity of silicone oil is 100 cSt, the squeeze speed is 10 μm/s, the initial gap distance is set at 0.625 mm, and the magnetic field is 0.46 T

The compression process could be divided into two regions: elastic deformation and plastic flow. At the elastic region, the particle chains or columns in the MR fluid keep intact without breaking. It bears the loading force by the elastic deformation of the particles. The normal force increase steeply from 3.38 to 8.45 N as the gap distance decreases or the stain increases to the critical value. The critical gap distance and strain is 0.622 and 0.008 mm, respectively. The further decreasing of the gap distance makes the MR fluid enter into the plastic flow. The particle chains structure collapses at a critical stress level and then immediately forms a metastable structure again. This process repeats as the compression proceeds and the normal forces increase slowly at first and then increase quickly to 29.8 N with decreasing of the gap distance (0.386 mm) or increasing of the strain (0.384). Besides, the increasing normal force with fluctuation can be found, which agrees well with the experimental (Chu et al. 2000) and simulated (Lukkarinen and Kaski 1998; de Vicente et al. 2011b) results. The fluctuation normal force is the macroscopic manifestation of the repeated microstructure in this plastic flow region. During this process, the average normal stress τ_N (defined by $\tau_N = F_N/A$, where A is the area of the plate) changes from 10.8 to 94.8 kPa, and the compressive yield stress (the transformation normal stress from the elastic region to the plastic region) is about 26.9 kPa which is much larger than the shear yield stress of 3.5 kPa (the shear yield stress is obtained by shear stress–shear rate plots and not shown here for brevity).

In the plastic flow region, the normal force (F_N) with the gap distance (h) can be fitted with a power law relation, which is $F_N \propto h^n$. In the log–log graph (Fig. 3c), a linear line with a slope of -2.4 is well used to capture the normal force with the gap at a constant field. The field-responsive fluid is usually regarded as homogenous material and modeled as simplified Bingham (Covey and Stanmore 1981; de Vicente et al. 2011b; Ruiz-López et al. 2012) or bi-viscous fluid (Lipscomb and Denn 1984; Gartling and Phan-Thien 1984; Williams et al. 1993). The continuum media theory shows that the normal forces vary with the gap distance in a power law relation. In the previous works, different power law indexes have been obtained (Meng and Filisko 2005; Lynch et al. 2006; McIntyre and Filisko 2010), and there exist some reasons to explain it. First, the field-responsive fluids are two-phase fluids consisting of particle aggregates immersed in a continuous liquid phase, not homogenous material. Second, the Bingham or bi-viscous model cannot fully describe the field-responsive fluid behaviors. Third, sealing effect exists, and it will increase the particle concentration of field-responsive fluid. Fourth, the squeeze strengthen effect will increase the yield stress of field-responsive fluid. Fifth, the slip may happen during the tests. These will be considered and discussed in detail later.

Magnetic field effect

Compression properties of MR fluids are highly dependent on the magnetic field (B). It should be remarked that magnetic field changes a little with the gap distance. Jonkkari et al. (2012) found that when the gap distance of the rheometer changed from 1.0 to 0.25 mm; the field decreased less than 4.5 % of the average field. The magnetic field may be regarded as constant value as the gap distance decreases, which is very different from the ER fluid whose field will increase greatly with decreasing of the gap distance when the constant voltage is applied. Different magnetic fields from 0.23 to 0.88 T are applied to show the field effect (Fig. 4). Under every given field distribution, the general feature of normal forces under compression can be found obviously. At the same gap distance, the normal force of MR fluid at high magnetic field is larger than that at low field, which is the typical MR effect. The increasing magnetic field strengthens the MR effect and the compressive stress of MR fluid. The compressive yield stress will be enhanced from 16.1 to 29.8 kPa as the magnetic field increases from 0.23 to 0.88 T. As magnetic field increases, the attractive force between the particles in the MR fluids increases; thus, the stronger chains which can bear larger loading force will form. Similar results have been obtained in previous researches (Mazlan et al. 2007, 2008; Wang et al. 2011; de Vicente et al. 2011b, Ruiz-López et al. 2012). However, the compressive yield stress does not show a quadratic relation with the magnetic field at high magnetic field as the magnetic saturation of the particle occurs.

In addition, the power law relation fitting is conducted for different fields, and the index changes between −2.40 and −2.59. Clearly, it does not always increase with increasing of the magnetic field, and at high magnetic field, it always keeps a minimum value. The similar phenomena can be found for other samples and compression conditions. Under a high magnetic field, the sealing effect will be more obvious, and more oil without particles would be squeezed out (Ismail et al. 2012). The particle concentration will increase and make the normal force grow faster during compressing.
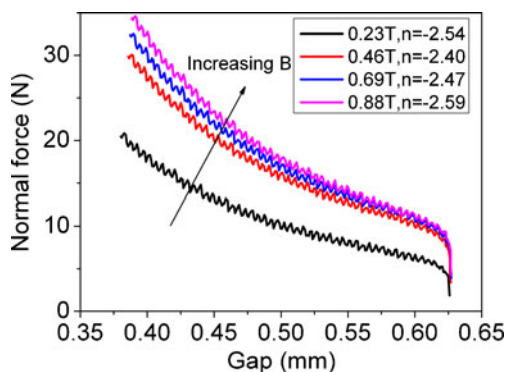
Compression velocity effect

Figure 5 shows the effect of compression velocity (V) on the MR fluid compression behavior. Four small velocities from 2 to 20 μm/s are tested (compressive rate range, 0.001–0.04 s^{-1}), and they are also believed to be quasi-static compression. At the same gap distance, the normal force increases as the compression velocity increases. The compressive yield stress is increased by a factor of 1.6 when the velocity changes from 2 to 20 μm/s. This is different from what has been found by McIntyre and Filisko (2010) for ER fluid under constant volume compression. They thought that the normal force of ER fluid decreased with increasing of the squeezing velocity. As in the filtration region, the reconstruction of particle structures would occur at an increasing rate as the compression speed decreased, and the stronger structures were formed at slower speeds. In the case of the MR fluids, these small compression velocities are much lower than the reconstruction rate of particle structure, and they have no much influence on the reconstruction of particle. As the compression velocity increases, the viscous drag force ($f_D = 3\pi\eta D_p V_p$, where D_p and V_p are the diameter and velocity of the particle, respectively) acting on the particles from carrier fluid becomes large, and larger normal force is needed to break the chains. Thus, the normal force increases with the increasing velocity. In addition, the compression velocity not only affects the normal force but also changes the power law index. The index decreases from −1.94 to −2.57 with the increased compression velocity from 2 to 20 μm/s. The normal forces increase faster at the high velocity than those at small high velocity.

Fig. 4 Normal forces with gap distance under different magnetic fields. The particle volume fraction of MR fluid is 10 %, the viscosity of silicone oil is 100 cSt, the squeeze speed is 10 μm/s, and the initial gap distance is set at 0.625 mm
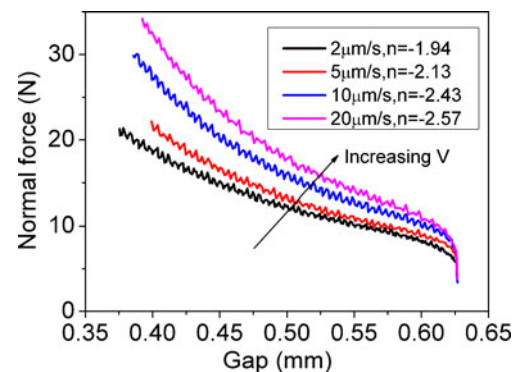
Fig. 5 Normal forces with gap distance under different compression velocities. The particle volume fraction of MR fluid is 10 %, the viscosity of silicone oil is 100 cSt, the initial gap distance is 0.625 mm, and the magnetic field is 0.46 T
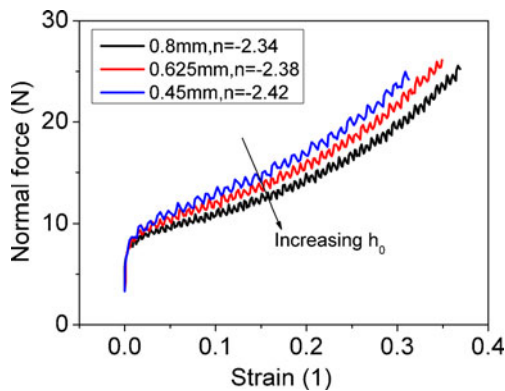
Fig. 6 Normal forces with compression strain under different initial gap distances. The particle volume fraction of MR fluid is 10 %, the viscosity of silicone oil is 100 cSt, the squeeze speed is 10 μm/s, and the magnetic field is 0.46 T

Fig. 7 Normal forces with gap distance for different particle volumes. The viscosity of silicone oil is 100 cSt, the initial gap distance is 0.45 mm, the squeeze speed is 10 μm/s, and the magnetic field is 0.23 T

Initial gap distance effect

Different initial gap distances ($h_0 = 0.45$, 0.625, and 0.8 mm) are tested to study the effect on the MR fluid compression behavior (Fig. 6). The normal force–strain plot is shown here in order to compare the normal force more directly. Obviously, smaller gap distance generates larger normal force at the same strain. The particle chains in the MR fluid can be seen as slim rods. According to the mechanics of compressing slim rods, the rod strength P_L is determined by the rod length l and rod diameter D by the following equation: $P_L = k_G D^2/l^2$, where k_G is a material parameter, which should be tightly related to the particle interactions (Timoshenko and Young 1968; Tian et al. 2003). The diameter of the chain varies with the length as $D \sim l^s (s < 1)$, where the value of s can be different for magnetically saturated particles and magnetically unsaturated particles (Zhou et al. 1998). Thus, the rod strength has a relation with the length as $P_L \sim l^{-2(1-s)}$. As the gap distance increases, the chain capacity of bearing loading force would weaken, and the normal force decreases. Besides, the power law index increases a little as the initial gap distance decreases. Obviously, for the high-concentration MR fluids, the particles form a more intricate network, but not simple chain or column. However, the rod buckling theory can also be utilized to explain the normal force with initial gap distance qualitatively.

Particle volume concentration effect

Compression behaviors for MR fluids with different particle concentration (φ) are compared in Fig. 7. The particle volume concentration increases from 5 to 25 %, and higher-concentration sampler has not been tested because the normal forces exceed the instrument test range (50 N). At the
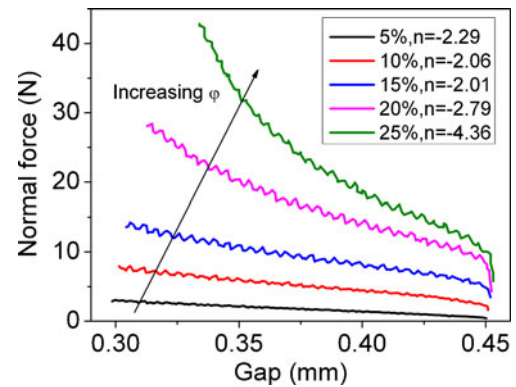
same gap distance, the normal force increases as the particle concentration increases. It is easy to understand that as the volume concentration of the iron particles increases, the interparticle distance decreases, which can enhance the particle interaction. Therefore, larger attractive force will be achieved among the particles, which enables the formation of more rigid structures in the suspension. They give rise to higher normal stresses as the particle volume concentration increases. The similar results have been obtained by de Vicente et al. (2011b), Ruiz-López et al. (2012). As shown in Fig. 8, the compressive yield stress increases from 1.6 to 31.8 kPa as the volume fraction increases from 5 to 25 %, which is a more clear evidence for the formation of stronger structures in more concentrated suspensions. Besides, the compressive yield stress increases proportionally with the volume fraction, which is $\tau_{CY} \propto \varphi$. The similar phenomenon also has been found for the shear yield stress with the volume concentration at the small concentration, but this relation is different from what have been obtained by Ruiz-López et al. (2012), where the experiments were made under constant volume squeeze flow.
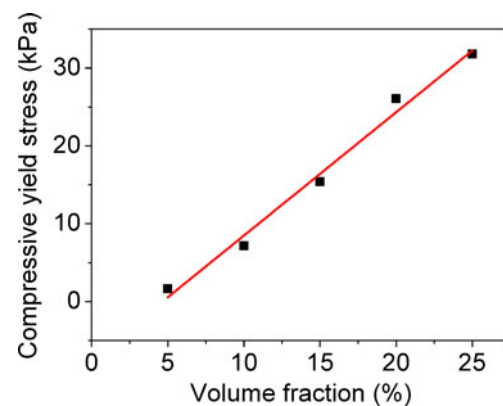
Fig. 8 Compressive yield stress varies proportionally with the volume fraction

The variation of the power law indexes of the low-concentration MR fluids from 5 to 20 % is small, and the index value changes between −2.8 and −2. However, for the 25 % MR fluid, the index reaches as low as −4.36, which is much smaller than those above. The normal force of the high-concentration MR fluid increases faster than the low-concentration sample. During compressing, the sealing effect will increase the particle concentration of MR fluid residues in the plate. The high-concentrated MR fluid will become even more concentrated with decreasing of the gap distance. It will enhance the interparticle force and form stronger particle structure, which greatly enhance the normal force.

Viscosity effect

The effect of viscosity (η) of carrier fluid on the compression behaviors of MR fluids is also studied in Fig. 9. Silicon oil with three viscosities of 10, 100, and 500 cSt was adopted, and MR fluid with larger viscosity will produce the normal force beyond the testing range. The normal force increases greatly as the viscosity of carrier fluid increase at the same gap distance, which is similar to the results (Ruiz-López et al. 2012). For example, the normal force increases from 10.66 to 29.16 N when the viscosity of the carrier fluid increases from 10 to 500 cSt at the gap distance of 0.5 mm. For MR fluids with carrier fluid of high viscosity, larger force will be needed to surpass the viscous drag force and the magnetic attractive force to break the formed particle structure, which means that the high viscosity carrier fluid can sustain the particle structure more effectively.

The power law index decreases with increasing of the viscosity of the carrier fluid, which is related to the sealing effect. During compressing, the particle and oil are both squeezed out, but high viscosity carrier fluid will take more particles, and it will decrease the changing of the particle
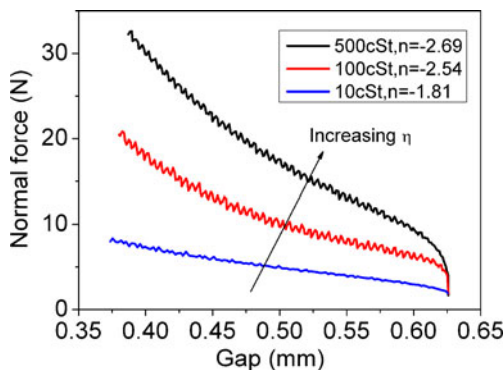
concentration for the MR fluid in the plate. So, the particle concentration for MR fluid with the high-viscosity carrier fluid is smaller than that with low-viscosity carrier fluid, and the normal force will increase slowly. It also shows that MR fluid with low-viscosity carrier fluid has more obvious sealing effect.

To sum up, the compressive stress is much larger than the shear stress, which makes MR fluid have great potential in vibration isolation. The fluctuation normal force under compressing would be harmful to vibration control and should be inhibited. High magnetic field, high compression velocity, low initial gap distance, high particle concentration, and high viscosity of carrier fluid would generate larger normal forces. Two regions were found through the normal force versus gap distance curves: elastic deformation and plastic flow. In the plastic flow region, the normal force with the gap distance could be fitted with a power law relation $F_N \propto h^n$, and the index n was around well in the range $(−3, −2)$.

Discussion

Comparison under the uniform and nonuniform fields

The compression flow of inelastic yield stress fluids was firstly studied by Scott (1929). Later, Covey and Stanmore (1981) reported the theoretical results by employing Bingham constitutive equation and the lubrication approximation; though their theoretical works were in some conflict with regard to the flow pattern produced in the geometry, they can provide the accurate and useful first-order estimate for the velocity field (Lipscomb and Denn 1984; Engmann et al. 2005). Furthermore, Gartling and Phan-Thien (1984) utilized a bi-viscous mode to carry out the theoretical analysis, and then Williams et al. (1993) adopted this method to calculate a time-dependent sinusoidal squeeze flow theory for ER fluids. Besides, de Vicente et al. (2011b), Ruiz-López et al. (2012) have proven the validity of continuous media theory for Bingham plastic material in MR fluids under slow compression. Following these methods, the theoretical model is developed taking magnetic field distribution into account.

In this case, the Reynolds number $R_e = h_o V \rho / \eta$ (where the characteristic length scale is the initial gap distance h_0; the characteristic velocity is chosen to be the squeezing velocity of the upper plate V, ρ and η is the density and viscosity of MR fluid, respectively) is an order of 10^{-4} and is much less than 1; lubrication and creeping flow approximations can be used. Besides, as the gap distance is small compared to the radius of the plate ($R > 10 h$), the normal component is neglected. Because of circular symmetry, the θ component is zero. The momentum balance equation in

Fig. 9 Normal forces with gap distance for different viscosities of carrier fluid. The particle concentration is 10 %, the initial gap distance is 0.625 mm, the squeeze speed is 10 μm/s, and the magnetic field is 0.23 T

cylindrical coordinate (r, θ, and z) can simplify just in the r component as follows:

$$-\frac{\partial p}{\partial r} + \frac{\partial \tau_{rz}}{\partial z} + \mu_0 M_r \frac{\partial H_r}{\partial r} = 0 \qquad (1)$$

where p is the total pressure, τ_{rz} is the shear stress, M_r is the fluid magnetization in the r component, and μ_0 is the vacuum magnetic permeability. The added third part of the left side of the equation is a magnetic body force arising from the radial magnetic field distribution H_r (Rosensweig 1997; López-López et al. 2010; Andablo-Reyes et al. 2011).

The bi-viscous model is chosen to represent constitutive relation for the plastic flow. Later, it can be seen that it would not affect the result too much compared to Bingham model. The bi-viscous model is given by the following equations:

$$\tau(H) = \tau_0(H) + \eta \frac{\partial U_r}{\partial z}, \text{ for } \tau^2 > \tau_1^2 \qquad (2a)$$

$$\tau(H) = \eta_r \frac{\partial U_r}{\partial z}, \text{ for } \tau^2 < \tau_1^2 \qquad (2b)$$

There are two shear stress τ_0 and τ_1, and τ_1 is the shear yield stress. η is the slope of the shear stress–shear rate curve above the yield point, and η_r is a viscosity parameter which is assigned to the fluid below yield. U_r is the fluid velocity. A new dimensionless parameter, the viscosity ratio, is defined by $\varepsilon = \eta/\eta_r$. Besides, $\tau_0 = \tau_1(1 - \varepsilon)$ can be obtained. The Bingham model is approached in the limit $\varepsilon \to 0$.

Because of symmetry, restricting attention is paid to the region $0 < z < h/2$, $0 < r < R$. Equation (1) can be rewritten as follows:

$$\frac{\partial}{\partial z}\tau = \frac{\partial p}{\partial r} - \mu_0 M_r \frac{\partial H_r}{\partial r} = \Phi(r) \qquad (3)$$

Generally $\Phi(r) < 0$. According to the boundary condition $z = h/2$, $\tau = 0$, and integrating Eq. (3) with respect to z produces the following equation:

$$\tau = \Phi(r)\left(z - \frac{h}{2}\right) \qquad (4)$$

From $\tau = \tau_1$, we get $z_y = \frac{h}{2} + \tau_1 \Phi^{-1}(r)$ which describes the vertical location of the boundary separating yielded material ($0 < z < z_y$) from unyielded material ($z < z_y < h/2$). Equations (2a) and (4) can be combined and integrated (no slip condition $z = 0$; $U_r = 0$) with respect to z to produce a velocity profile for the yielded material as follows:

$$U_{r1} = \frac{1}{2\eta}\Phi(r)(z - h)z - \frac{\tau_0(H)}{\eta}z, \quad 0 \le z \le z_y \qquad (5)$$

Similarly, the velocity of the unyielded material, U_{r2}, which is found by combining Eqs. (2b) and (4) and integrating with respect to z. The constant of integration is found by

matching the velocities U_{r1} and U_{r2} at the yield surface $z = z_y$. It produces the result as follows:

$$\begin{aligned} U_{r2} = & \frac{1}{2\eta_r}\Phi(r)(z - h)z \\ & + \left(\frac{1}{2\eta} - \frac{1}{2\eta_r}\right)\Phi(r)(Z_y - h)Z_y \\ & - \frac{\tau_0(H)}{\eta}Z_y, \quad Z_y \le z \le \frac{h}{2} \end{aligned} \qquad (6)$$

Taking a mass balance over a cylinder confined by a radius r and the planes $z = 0$, $z = h/2$, we have $\pi r^2 d(\frac{h}{2})/dt = 2\pi r \int_0^{h/2} U_r dz$. In constant velocity squeeze, it can be rewritten as follows:

$$\frac{rV}{4} = \int_0^{h/2} U_r dz = \int_0^{Z_y} U_r dz + \int_{Z_y}^{h/2} U_r dz \qquad (7)$$

Combining this with Eqs. (5) and (6) gives an expression for $\Phi(r)$, i.e., as follows:

$$\begin{aligned} \eta_r h^3 \Phi^3 + 3\eta_r \tau_0 h^2 \Phi^2 + 6\eta\eta_r r V\Phi^2 - 8\eta\tau_1^3 - 12\eta_r\tau_0\tau_1^2 \\ + 8\eta\tau_1^3 = 0 \end{aligned} \qquad (8)$$

The dimensionless parameters X (analogue of the dimensionless pressure gradient) and S (modified plasticity number) are introduced as follows:

$$X = -\frac{h}{2\tau_1}\Phi, \quad S = \frac{r\eta V}{h^2 \tau_1} \qquad (9)$$

The expression then becomes the following equation:

$$X^3 - 3\left(S + \frac{1}{2}\right)X^2 + \frac{1}{2} = \varepsilon\left(\frac{1}{2} - \frac{3}{2}X^2\right) \qquad (10)$$

This expression is very similar to those obtained by Williams et al. (1993), and the only difference is that the dimensionless parameter X includes the contribution from the magnetic field. The exact solution of Eq. (10) could be acquired by the mathematical software, but it is very tedious and complicate, which cannot give the straightforward understanding. In order to directly show the effect of the magnetic field distribution on the normal force, the approximate solution is developed. For the MR fluid, the viscosity ratio $\varepsilon \sim 10^{-4} < 1$, and Eq. (10) can be simplified as follows:

$$X^3 - 3\left(S + \frac{1}{2}\right)X^2 + \frac{1}{2} = 0 \qquad (11)$$

It is the result obtained by Bingham model. Bingham and bi-viscous models have no too much difference in this case for the MR fluid. Besides, $z_y = \frac{h}{2} + \tau_1 \varphi^{-1}(r) > 0$ is needed in physics; so, $X = -\frac{h}{2\tau_1}\varphi > 1$. The plastic number for the MR fluid is less than 0.05, and the solution of Eq. (11) can be obtained by the following equation:

$$X = 1 + \sqrt{2S} \qquad (12)$$

Substituting it by Eq. (9), it produces the following expression:

$$\frac{\partial p}{\partial r} = -\frac{2\tau_1(H)}{h} - \frac{2\tau_1(H)}{h^2}\left(\frac{2r\eta V}{\tau_1(H)}\right)^{1/2} + \mu_0 M_r \frac{\partial H_r}{\partial r}$$

$$(13)$$

Then, neglecting the atmosphere pressure and integrating the pressure over the total plate area gives the following expression:

$$
\begin{aligned}
F_N &= \int_0^R 2\pi p(r)r\,dr = -\pi \int_0^R \frac{\partial p(r)}{\partial r}r^2\,dr \\
&= \frac{2\pi}{h}\int_0^R \tau_1(H)r^2\,dr + \frac{2\pi}{h^2}(2\eta V)^{1/2} \\
&\quad \times \int_0^R \tau_1^{1/2}(H)r^{5/2}\,dr - \pi_0\mu_0 \int_0^R M_r \frac{\partial H_r}{\partial r}r^2\,dr
\end{aligned}
$$

$$(14)$$

If the magnetic field is constant along the radial displacement, the compression normal force can be obtained as follows:

$$F_N = \frac{2\pi\tau_1 R^3}{3h} + \frac{4\pi}{7h^2}\sqrt{2\tau_1\eta V R^7}$$

$$(15)$$

It should be noted that the forces in the Eqs. (14) and (15) do not contain the static normal force F_{NS}. The biggest difference between uniform [Eq. (15)] and nonuniform magnetic field [Eq. (14)] is the magnetic field gradient-induced normal force, which is the third part of the left side of Eq. (15). Here, M_r is the r component of the fluid magnetization. The MR fluid is considered as an anisotropic medium, and the magnetization is a function of magnetic field $M_r = \chi_{rz}H_{zz}$, where H_{zz} is the z component of applied magnetic field ($H_{rr} = H_{\theta\theta} = 0$), and χ_{rz} is the magnetic susceptibility of the fluid. The chains or columns formed in the fluid will be coarsening during compressing. Thus, the magnetic susceptibility will be changed. If the change is ignored, the magnetic susceptibility χ_{rz} is regarded as a constant value. Moreover, the magnetic field distribution is also considered as the steady value with decreasing of the gap distance, so the force produced by third part due to the field gradient will keep a steady value during compressing, which is independent on the gap distance h.

The other difference between the uniform and nonuniform field is the shear yield stress along the radial displacement. The shear yield stress is a function of magnetic field, and it is a constant value for the different radial displacements under uniform magnetic field. However, the magnetic field along the radial displacement is different under nonuniform field; the shear stress cannot keep constant, and integration for the normal force is needed. For the 10 % MR fluid with 100 cSt, the normal forces in the nonuniform and uniform field are compared. The shear

stress is measured with the plate–plate magneto-rheometer under different fields, and Bingham model is used to fit the data. The shear stress–shear rate curves show that the initial viscosity of the fluid is 0.24 Pa/s, and the shear yield stress with magnetic field is fitted with polynomial function $\tau_1(B) = 4{,}680.8B^3 - 12{,}537B^2 + 12{,}595B - 11.617$. Supposing χ_{rz} is 1 and neglecting the static normal force, the normal forces from Eqs. (14) and (15) can be calculated by the following expressions:

$$F_N(N) = \frac{7.658}{h\,(mm)} + \frac{0.023}{h^2\,(mm)} + 0.34, \text{ nonuniform field}$$

$$(16)$$

$$F_N(N) = \frac{7.74}{h\,(mm)} + \frac{0.024}{h^2\,(mm)}, \text{ uniform field}$$

$$(17)$$

The magnetic field distribution comes from the Fig. 1b of the paper by López-López et al. (2010). As shown in Fig. 10, the normal forces calculated under nonuniform and uniform field and experimental results are compared in the plastic region. The indexes in the nonuniform and uniform field are slightly different, both around −1.0. The normal forces under nonuniform field are larger than those in uniform field, as it produces the magnetic field gradient-induced force. In order to obtain the accurate normal force under compression, it is very necessary to consider the nonuniform field, especially at the condition where the magnetic field changes sharply. However, the calculated and experimental values do not agree well. On the one hand, the calculated initial normal force is larger than the experimental one, which may arise from the shear yield stress measured by the rheometer under nonuniform field. A local distinct maximum of magnetic flux density at the sample rim gives rise to ponderomotive forces, which make the carbonyl iron particle migrate towards the maximum of the flux density.
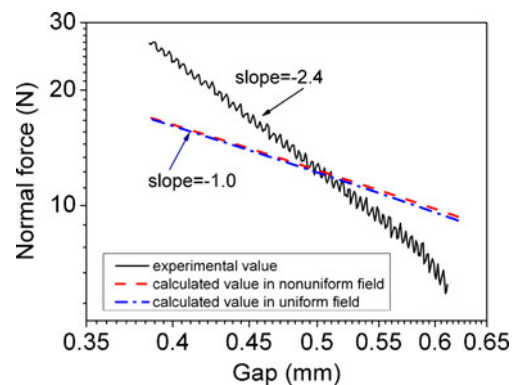
Fig. 10 Comparison of normal forces between the experimental and theoretical results. The particle volume fraction of MR fluid is 10 %, the viscosity of silicone oil is 100 cSt, the squeeze speed is 10 μm/s, the initial gap distance is set at 0.625 mm, and the magnetic field is 0.46 T

This particle migration will cause a radial profile of particle concentration, exhibiting a distinct maximum at the rim and further increase the shear stress. That is, the measured shear yield stress is much larger than the true yield stress (Laun et al. 2008a, b), which makes the calculated initial normal force larger than the experimental value. Besides, the particle migration will also change the homogeneity and compression behavior of MR fluid.

On the other hand, the index of the normal force with the gap distance for theory and testing is also different. Obviously, the compression forces are predominated by the shear yield stress, and viscous force has little contribution. The Eqs. (16) and (17) can be both approximated as $F_N \propto h^{-1}$. In this case, this theoretical value of about -1 is much larger than the experimental value of -2.40 for the index of power law relation. There must be another reason to lead the deviation.

Gap distance-dependent shear yield stress

The huge difference between the theoretical and experimental values may also come from the shear yield stress, which is regarded as the gap distance-independent value during the above calculation. However, there exist two influencing factors changing the yield stress during compressing: sealing effect and squeeze strengthening effect. First, the sealing effect will happen (Chu et al. 2000; Meng and Filisko 2005; Lynch et al. 2006; McIntyre and Filisko 2010) and increase the volume concentration of the particle which leads the increasing of the shear yield. Both microscopic and macroscopic models predict that the yield stress is proportional to the volume fraction of particle loading at lower volume fraction, which is $\tau_y \sim \varphi$ (Shulman et al. 1986; Ginder and Davis 1994). At higher volume fraction, the yield stress increases faster. For most practical MR fluids which have a high volume fraction, the relationship of the yield stress and volume fraction is usually represented by a power law $\tau_y \sim \varphi^m$ ($m = 1.52$) (Carlson 2005). At the extreme condition, only the clean oil is expelled out, while the iron particles fully stay between the plates under compression. The volume fraction for the MR fluid in the plate can be calculated as $\varphi = h_0 \varphi_0 / h$ (φ_0 is the initial volume fraction). Therefore, the yield stress increase with decreasing of the gap distance, and the relation between them can be expressed as $\tau_y \sim h^{-\alpha}$, where α is related to the sealing effect. Second, the squeeze strengthening effect would increase the shear stress. Tang et al. (2000) have proposed that the yield stress increases proportionally with increasing of the normal stress, that is $\tau_y \propto P_e$, in which the $P_e = F_N / A$ is the normal stress loading on the MR fluid. The normal force under compression increases with decreasing of the gap distance, so the normal stress loading on the MR fluid will increase, and this will lead to the increasing of the shear

yield stress. In this case, the gap distance-dependent squeeze yield stress may be simplified as $\tau_y = \tau_{y0}(h_0/h)^\beta$, where τ_{y0} is the yield stress of MR fluid without compression, and β is relative to the squeeze strengthening effect. Therefore, the shear yield stress will increase with decreasing of the gap distance.

During compressing, the squeeze strengthening effect on increasing the yield stress will always exist, and the sealing effect can also happen, but not always at the extreme condition (the iron particle will be squeezed partially). Neglecting the viscous effect and substituting the gap distance-dependent shear yield stress into the normal force expression under uniform field gives the following expression:

$$F_N \in \left[\frac{A}{h^{1+\beta}}, \frac{B}{h^{1+\alpha+\beta}} \right] \tag{18}$$

where A and B are constant values, which relative the compression material and conditions. The normal force is decided by these two effects, but the determinate normal force which is very hard to be decided as the degree of the sealing effecting is unknown. Thus, the normal force will be in the range of two extreme conditions: homogenous compression (oil and particle are not separated, and both of them are squeeze out proportionally) and extreme compression (oil and particle are fully separated, and only oil is squeezed out).

In the certain condition, the sealing effect and squeeze strengthening effect play determinate roles. Thus, the normal force will linearly change with the gap distance in the log–log plot, and a constant index of power law relation will be acquired. As the compression condition changes, the index will change in the range of $[-(1 + \beta), -(1 + \alpha + \beta)]$. For example, as shown in Fig. 4, the index will change as the magnetic field increases. It is because that the sealing effect will be changed under various magnetic fields. As the magnetic field increases, the iron particle attractive force is increased, and it makes the particle hard to be squeezed out. The sealing effect will be more severe at high field, and the index will become much smaller than that at low field.

Conclusions

This work studied the normal force of MR fluids under compression by a commercial plate–plate rheometer, where the magnetic field along the radial displacement is nonuniform. The normal stress of MR fluids under compression is larger than that in shear or valve mode, and it increases with decreasing of the gap distance. The gap distance-dependent normal force of MR fluid can be divided into two regions: elastic deformation and plastic flow. The normal force with the fluctuation is found at the plastic flow region. A power

law relation $F_N \propto h^n$ is utilized to capture the normal force with the gap distance in this region. The index of the power law relation is around well in the range $(-3, -2)$ and will change a little with different MR samples and compression conditions. High magnetic field, high compression velocity, low initial gap distance, high volume fraction, and high medium viscosity will produce large normal force at the same gap distance or strain during the compressing.

Based on the continuum media theory, the theoretical model is developed to calculate the normal force under the nonuniform field. Compared to that under uniform field, the magnetic field gradient-induced normal force cannot be neglected. The shear yield stress along the radial displacement will also be changed under the nonuniform field. However, the index of the power law relation obtained by the experimental result is much smaller than that by the theoretical prediction. Considering the sealing effect and squeeze strengthening effect, the gap distance-dependent shear yield stress is proposed to calculate the normal forces. A range is obtained for the normal force between the homogenous and extreme compression, and good agreement is obtained between the experimental and theoretical results.

References

Andablo-Reyes E, Hidalgo-Álvarez R, de Vicente J (2011) Controlling friction using magnetic nanofluids. Soft Matter 7:880–883

Ashour O, Rogers CA, Kordonsky W (1996) Magnetorheological fluids: materials, characterization, and devices. J Intell Mater Syst Struct 7:123–130

Bossis G, Volkova O, Lacis S, Meunier A (2002) Magnetorheology: fluids, structures and rheology. Lecture notes in physics. Springer, Berlin

Carlson JD (2005) MR fluids and devices in the real world. Int J Mod Phys B 19:1463–1470

Carlson JD, Jolly MR (2000) MR fluid, foam and elastomer devices. Mechatronics 10:555–569

Chu SH, Lee SJ, Ahn KH (2000) An experimental study on the squeezing flow of electrorheological suspensions. J Rheol 44(1):105–120

Covey GH, Stanmore BR (1981) Use of the parallel-plate plastometer for the characterization of viscous fluids with a yield stress. J Non-Newton Fluid Mech 8:249–260

de Vicente J, Klingenberg DJ, Hidalgo-Álvarez R (2011a) Magnetorheological fluids: a review. Soft Matter 7:3701–3710

de Vicente J, Ruiz-López JA, Andablo-Reyes E, Segovia-Gutiérrez JP, Hidalgo-Álvarez R (2011b) Squeeze flow magnetorheology. J Rheol 55:753–779

Engmann J, Servais C, Burbidge AS (2005) Squeeze flow theory and applications to rheometry: a review. J Non-Newton Fluid Mech 132:1–27

Farjoud A, Craft M, Burke W, Ahmadian M (2011) Experimental investigation of MR squeeze mounts. J Intell Mater Syst Struct 22:1645–1652

Farjoud A, Mahmoodi N, Ahmadian M (2012) Nonlinear model of squeeze flow of fluids with yield stress using perturbation techniques. Mod Phys Lett B 1150040:26

Gartling DK, Phan-Thien N (1984) A numerical simulation of a plastic fluid in a parallel-plate plastometer. J Non-Newton Fluid Mech 14:347–360

Ginder JM, Davis LC (1994) Shear stresses in magnetorheological fluids: role of magnetic saturation. Appl Phys Lett 65(26):3410–3412

Gong XL, Guo CY, Xuan SH, Liu TX, Zong LH, Peng C (2012) Oscillatory normal forces of magnetorheological fluids. Soft Matter 8:5256–5261

Gstöttenbauer N, Kainz A, Manhartsgruber B, Scheidl R (2008) Experimental and numerical studies of squeeze mode behaviour of magnetic fluid. Proc IMechE C 222:2395–2407

Havelka KO, Pialet JW (1996) Electrorheological technology: the future is now. Chemtech 36:36–45

Ismail I, Mazlan SA, Zamzuri1 H, Olabi AG (2012) Fluid-particle separation of magnetorheological fluid in squeeze mode. Jpn J Appl Phys 067301:51

Jonkkari I, Kostamo E, Kostamo J, Syrjala S, Pietola M (2012) Effect of the plate surface characteristics and gap height on yield stresses of a magnetorheological fluid. Smart Mater Struct 21:075030

Kulkarni P, Ciocanel C, Vieira SL, Naganathan N (2003) Study of the behavior of MR fluids in squeeze, torsional and valve modes. J Intell Mater Syst Struct 14:99–104

Laeuger J, Wollny K, Stettin H, Huck S (2005) A new device for the full rheological characterization of magneto-rheological fluids. Int J Mod Phys B 19:1353–1359

Laun HM, Schmidt G, Gabriel C (2008a) Reliable plate-plate MRF magnetorheometry based on validated radial magnetic flux density profile simulations. Rheol Acta 47:1049–1059

Laun HM, Gabriel C, Schmidt G (2008b) Primary and secondary normal stress differences of a magnetorheological fluid (MRF) up to magnetic flux densities of 1 T. J Non-Newton Mech 148:47–56

Lipscomb GG, Denn MM (1984) Flow of Bingham fluids in complex geometries. J Non-Newton Fluid Mech 14:337–346

López-López MT, Kuzhir P, Durán JDG, Bossis G (2010) Normal stresses in a shear flow of magnetorheological suspensions: viscoelastic versus Maxwell stresses. J Rheol 54:1119–1136

Lukkarinen A, Kaski K (1998) Simulation studies of electrorheological fluids under shear, compression, and elongation loading. J Appl Phys 83:1717–1725

Lynch R, Meng Y, Filisko FE (2006) Compression of dispersions to high stress under electric fields: effects of concentration and dispersing oil. J Colloid Interface Sci 297:322–328

Mazlan SA, Ekreem NB, Olabi AG (2007) The performance of magnetorheological fluid in squeeze mode. Smart Mater Struct 16:1678–1682

Mazlan SA, Ekreem NB, Olabi AG (2008) An investigation of the behaviour of magnetorheological fluids in compression mode. J Mater Process Technol 201:780–785

McIntyre EC, Filisko FE (2010) Filtration in electrorheological suspensions related to the Peclet number. J Rheol 54(3):591–603

Meng Y, Filisko FE (2005) Unidirectional compression of electrorheological fluids in electric fields. J Appl Phys 98:074901

Park BJ, Fang FF, Choi HJ (2010) Magnetorheology: materials and application. Soft Matter 6:5246–5253

Rosenweig RE (1997) Ferrohydrodynamics. Dover, New York

Ruiz-López JA, Hidalgo-Alvarez R, de Vicente J (2012) On the validity of continuous media theory for plastic materials in magnetorheological fluids under slow compression. Rheol Acta 51:595–852

See H (2003a) Field dependence of the response of a magnetorheological suspension under steady shear flow and squeezing flow. Rheol Acta 42:86–92

See H, Tanner R (2003b) Shear rate dependence of the normal force of a magnetorheological suspension. Rheol Acta 42:166–170

Shulman ZP, Kordonsky VI, Zaltsgendler EA, Prokhorov IV, Khusid BM, Demchuk SA (1986) Structure, physical properties and dynamics of magnetorheological suspensions. Int J Multiph Flow 12:935–955

Scott JR (1929). Trans Inst Rubber Ind 4:347–347

Tang X, Zhang X, Tao R, Rong Y (2000) Structure-enhanced yield stress of magnetorheological fluids. J Appl Phys 87(5):2634–2638

Tian Y, Meng Y, Mao H, Wen S (2002a) Electrorheological fluid under elongation, compression, and shearing. Phys Rev E 65:031507

Tian Y, Meng Y, Mao H, Wen S (2002b) Mechanical property of electrorheological fluid under step compression. J Appl Phys 92:6875–6879

Tian Y, Wen S, Meng Y (2003) Compressions of electrorheological fluids under different initial gap distances. Phys Rev E 67:051501

Timoshenko S, Young DH (1968) Elements of strength of materials. D Van Nostrand, Princeton

Vieira SL, Ciocanel C, Kulkarni P, Agrawal A, Naganathan N (2003) Behaviour of MR fluids in squeeze mode. Int J Veh Des 33:36–49

Wang H, Bi C, Kan J, Gao C, Xiao W (2011) The mechanical property of magnetorheological fluid under compression, elongation, and shearing. J Intell Mater Syst Struct 22:811–816

Williams EW, Rigby SG, Sproston JL, Stanway R (1993) Electrorheological fluids applied to an automotive engine mount. J Non-Newton Fluid Mech 47:221–238

Zhang XJ, Farjoud A, Ahmadian M, Guo KH, Craft M (2011) Dynamic testing and modeling of an MR squeeze mount. J Intell Mater Syst Struct 22:1717–1728

Zhang XZ, Gong XL, Zhang PQ, Wang QM (2004) Study on the mechanism of the squeeze-strengthen effect in magnetorheological fluids. J Appl Phys 96(4):2359–2364

Zhou L, Wen W, Sheng P (1998) Ground states of magnetorheological fluids. Phys Rev Lett 81:1509–1512